Discovery of succinate dehydrogenase candidate fungicides via lead optimization for effective resistance management of *Fusarium oxysporum* f. sp. *capsici*

Sehrish Iftikhar
University of the Punjab
Louis Bengyella (bengyellalouis@gmail.com)
Pennsylvania State University Altoona: Penn State Altoona https://orcid.org/0000-0002-4823-5947
Ahmad Ali Shahid
University of the Punjab
Kiran Nawaz
University of the Punjab
Waheed Anwar
University of the Punjab
Sajid Ali
University of the Punjab

Research Article

Keywords: SdhI-resistance, penthiopyrad, fungicide, Fusarium wilt, chili rot disease control, docking, and virtual screening.

Posted Date: June 2nd, 2021

DOI: https://doi.org/10.21203/rs.3.rs-549182/v1

Version of Record: A version of this preprint was published at 3 Biotech on March 28th, 2022. See the published version at https://doi.org/10.1007/s13205-022-03157-8.

Abstract

Fusarium wilt of chili caused by the fungus *Fusarium oxysporum* f. sp. *capsici* (FCO) severely reduces the production of chili worldwide. There is growing evidence of resistance to commercial fungicides targeting succinate dehydrogenase (Sdh) of FCO soliciting the development of new Sdh inhibitors (SdhIs). In the current work, optimize docking and virtual screening were used to mine twelve SdhIs from the ZINC database, followed by *in vitro* antifungal evaluation on spore and radial mycelium development. Four new promising SdhIs exhibiting a mean mycelium inhibition rate greater than 85.6% (F = 155.8, P = 0.001, $P < 0.05$) were observed on ten strains of virulent resistant FCO. Importantly, three of the discovered molecules exhibited potent spore germination inhibition (≥ 80%, P = 00.1, $P < 0.05$) compared to the commonly used fungicide penthiopyrad. A significant positive correlation ($r^* \geq 0.67$, $P < 0.05$) between the activities of the newly discovered SdhIs compared to penthiopyrad against all tested FCO strains indicated a broad-spectrum fungicidal activity. The current findings indicate that the four SdhI's discovered could judiciously replace certain commercial SdhIs displaying resistance against *F. oxysporum* f. sp. *capsici*.

1. Introduction

Chili pepper (*Capsicum annum* L.) is considered as one of the most important vegetable crops farmed over 19.89 million hectares with an annual output of 33.52 million tons worldwide (Patel et al. 2014). Chili pepper production stands at 2.31 tons/hectare per annum in Pakistan contributing significantly to the economy (Khan et al. 2017; Nawaz et al. 2018a). Over the years, chili pepper production area in Pakistan shrunk by 2.68% from 64,175 ha in 2007 to an estimated 62,456 ha (Khan et al. 2017). Because land infestation by soilborne pathogens is difficult to manage by crop rotation, raised beds, water management, and fungicides application have compelled farmers to abandon chili farmland (Nawaz et al. 2018a). Root-rot and collar-rot diseases of chili pepper induced by the oomycete – *Phytophthora capsici* (Nawaz et al. 2018a; Nawaz et al. 2018b), die-back and fruit rot caused by *Colletotrichum* species in chili pepper (Khaleeque et Khan 1991), and *Fusarium* wilt of chili pepper (Skaggs et al. 2000) are widely reported in Pakistan. Among these groups of fungal diseases, *Fusarium* wilt of chili pepper incited by the soilborne *Fusarium oxysporum* (Schlect.) emend. Synd. and Hans. f. sp. capsici (FCO) is one of the most severe plant diseases worldwide.

FCO incites vascular and root wilts, vein clearing in younger leaflets, epinasty, stunting, yellowing of older leaves, and progressively colonized xylem tissues and disrupt translocation of nutrients leading to death (Agrios 2005; Siddiqui and Akhtar 2007). In Pakistan, *Fusarium* wilt of chili pepper causes an estimated 10–50% of the total yield losses (Siddiqui and Akhtar 2007; Irum 2007; Bashir et al. 2017). In horticultural practices, concurrent use of synthetic fungicides, grafting, and cultural practices variably control FCO and also lead to the emergence of virulent strains that are resistant to conventional fungicides (Akuram et al. 2018). Thus, there is a need to develop strategies to counter the FCO fungicide resistance.

Introducing biocontrol agents such as *Trichoderma* species to curb fungal diseases of chili pepper and mitigate fungicide resistance in Pakistan has been initiated (Nawaz et al. 2018b). An alternative containment measure for FCO–fungicide resistance management could be the introduction of new or structurally diverse antifungal molecules for the following reasons: 1) to delay the onset of resistance and 2) to effectively control diseases as compounds with better binding conformation provide enhanced antifungal activity by specifically blocking other amino acid residues on the receptor site of the target protein. Carboxamide fungicides which inhibit succinate dehydrogenase (Sdh; EC 1.3.5.1) enzyme could be used as a target protein to control FCO (Thomas et al. 2014; Iftikhar et al. 2017). The FCO Sdh is universal and a multi-subunit enzyme at the crossways of tricarboxylic acid cycle (TCA) and electron transport chain (ETC) that catalyzes the oxidation of succinate into fumarate. Succinate dehydrogenase inhibitors (SdhIs) disrupt the ETC by binding to ubiquinone (UQ) site and effective for controlling fungal diseases of plants. With the prevalence of diverse virulent FCO and the emergence of resistance in chili farming region of Pakistan, finding an ideal fungicide that can control most of the resistant FCO strains would provide a durable solution in cutting down yield losses. The objective of this study was: 1) to mine candidate unreported SdhIs from the ZINC database, dock, and virtually screen for interaction with *F. oxysporum* f. sp. *capsici* Sdh, and 2) to evaluate the *in vitro* antifungal potential of candidate SdhIs at the level of mycelium and conidia. It was found that candidate SdhIs with ZINC accession numbers ZINC03102709, ZINC17007371, ZINC32180696, and ZINC00781454 were significantly active against resistant *F. oxysporum* f. sp. *capsici* compared to commercially fungicide–penthiopyrad.

2. Materials And Methods

2.1.1 Mining Sdh potential inhibitors

A pipeline was developed (Fig. 1) and a preliminary *in silico* screening was performed using 18 reference fungicides active ingredients viz., benodanil, benzovindiflupyr, bixafen, boscalid, fenfuram, fluopyram, flutolanil, fluxapyroxad, furametpyr, isofetamid, isopyrazam, mepronil, oxycarboxin, penflufen, penthiopyrad, sedaxane, and thifluzamide (Supplementary Fig. S1) from Fungicide Resistance Action Committee (FRAC group: 7) to interrogate the ZINC database (http://zinc.docking.org/). These active ingredients were screened for homologs in the ZINC database at default mode (Table 1). The 2D structures of generated homologous molecules were constructed and converted to 3D structures on ChemDraw Ultra v12.0 (Li et al. 2004). The 3D structures were energetically minimized using MOE suit v2009.10 (Molecular Operating Environment.2013.08) until the RMSD gradient of 0.05 kcal.mol^{-1}.Å^{-1} was reached (Fig. S2).

2.1.2 Pharmacophore generation and compound selection

Pharmacophore modeling was performed in order to screen for the output homologous drug-like compounds from the ZINC database as previously described (Irwin et al. 2012). Pharmacophore models were generated by superimposing the 3D structures of the 18 fungicides based on the positions of annotation points (such as aromatic center, H-bond donors and acceptors, and hydrophobic centers) for

the homologous fungicides using MOE suit v2009.10. To identify novel Sdh inhibitors, a set of 17,900,742 compounds were retrieved from ZINC database drug-like category. The drug-like categories were further screened by the pharmacophore model at default mode, retrieving 50,000 compounds which were subsequently subjected to the structure-based virtual screening (SBVS) protocol.

2.1.3 SBVS of 50,000 compounds by auto-dock tools

A library of 50,000 screened drug-like pharmacophore compounds was docked into the ubiquinone binding site of reference *Alternaria solani* Sdh by AutoDock Tools (ADT) v4.0 (Morris et al. 2009), given that Sdh enzyme for fungi is universal. The docking calculations were performed on Intel-Xeon-QuadTM core processor 3.0 GHz Linux workstation. AutoDock Tools v4.0 was used with empirical free energy function and a Lamarckian genetic algorithm (Morris et al. 2009). The polar hydrogen atoms and Kollman charges were added to the protein model. Partial charges of UQ were assigned with Gasteiger charges. The active site was defined on UQ binding site by AutoGrid. The grid size was 70 Å × 70 Å × 70 Å, grid spacing of 0.375 Å, step size of 1.0 Å for translation, 50 degrees for rotation, and a maximum number of energy evaluations was set at 250,000. A total of ten conformations were generated for each compound. The docked protein-ligand complexes were evaluated based on the interaction energy of each conformation for the compounds.

2.1.4 Re-scoring and lead optimization of compounds

From docking analysis, the top 500 molecules (≈1 %) were re-scored in MOE suit v2009 and a consensus score based on ADT and MOE scores was selected for visual inspection of the geometrical matching of ligands with residues of amino acids at the docking site. Molecules with inconsistent docking conformations were removed after visual inspection. From the pipeline, 25 molecules were generated as potential Sdh inhibitors but 12 out of the 25 molecules were already in the market. Thus, 12 uncommercialized molecules were synthesized by MolPort® (www.molport.com; Lacplesa iela, Rega, Lativa) and subjected to *in vitro* testing and bioassays.

2.1.5 Model building of Sdh for *Fusarium oxysporum* and template search

The UQ site is a hydrophobic cleft composed of the amino acid residues of Sdh-B, Sdh-C, and Sdh-D which are highly conserved among a wide range of organisms (Sun et al. 2005; Hwang et al. 2006). So, the Sdh model for *F. oxysporum* was constructed using different reference subunit sequences for *F. oxysporum* (Table S1). The SWISS-MODEL template library (SMTL version 2019-03-06, PDB release 2019-03-01) was searched with BLAST (Camacho et al. 2009), and HHBlits (Remmert et al. 2011), for evolutionary related structures matching the target sequence.

Template search with BLAST and HHBlits has was performed against the SWISS-MODEL template library (SMTL, last update: 2019-03-06, last included PDB release: 2019-03-01). The target sequence of four subunits was searched with BLAST against the primary amino acid sequence contained in the SMTL. An initial HHblits profile was built using the procedure outlined in Remmert et al. (2011), followed by 1

iteration of HHblits against NR20. The obtained profile was searched against all profiles of SMTL. A total of 32 templates were found.

2.1.6 Refined model building, quality estimation, and docking analysis

Models were built based on the target-template alignment using open ProMod3 (https://openstructure.org/promod3/1.3/). Coordinates that were conserved between the target and the template were copied from the template to the model. Insertions and deletions were re-modeled using a fragment library and side chains were rebuilt. Finally, the geometry of the resulting model was regularized by using a force field. In cases where loop modeling with ProMod3 failed, an alternative model was built with PROMOD-II (Guex et al. 1997).

To evaluate the internal reliability and consistency, the stereo-chemical properties of models based on energy minimization, refinement, a simulation program called PROCHECK v3.4.4 (Laskowski et al. 1993) was used. Furthermore, Ramachandran plot was used to assess whether the values of the dihedral Psi/Phi/Chi/Omega angels agree with the values of allowed conformation for protein backbones.

The drug discovery tool 1-Click Docking (Mcule Inc, https://mcule.com/apps/1-click-docking/) was used to dock the discovered compounds within the UQ site of *F. oxysporum* f. sp. *capsici* Sdh at the default setting. 1-Click docking uses Vina filter (Trott and Olsen 2010), and dock ligand into a single target specifying binding sites. Gasteiger charges and hydrogens were added in the input files; non-polar hydrogens, lone-pairs, and non-standard residues were removed. Molecular graphics and analyses were performed with the UCSF Chimera package (Petterson 2004).

2.2 Succinate dehydrogenase activity of *F. oxysporum* f. sp. *capsici*

To confirm that all fungal strains were actively producing succinate dehydrogenase (Sdh) and that the new molecules were specifically targeting the Sdh, a colorimetric assay was performed. Stock cultures of single spore of resistant and virulent *F. oxysporum* f. sp. *capsici* (FCO) viz., FCO1, FCO2, FCO3, FCO4, FCO5, FCO6, FCO7, FCO8, FCO9, and FCO10 were used. The FCO strains were grown for 5 days on Potato Dextrose Agar (PDA; Difco) in a 9 cm diameter Petri plates at 25°C, and 16 h photoperiod.

Succinate dehydrogenase (Sdh) activity was assessed with BioVision® colorimetric assay Kit 1/14 (BioVision Inc, Milpitas, CA, USA). Briefly, fungal mycelia (10 mg) were rapidly homogenized with 100 µL ice-cold Sdh assay buffer, kept on ice for 10 min and centrifuged at 10,000 ×g for 5 min. A 15 µL supernatant of the homogenate and 5 µL (10 µg/mL) of each synthesized compound mined from the *in-silico* pipeline (Fig. 1) was added. The volume of the reaction mixture was adjusted to 50 µL with Sdh assay buffer and transferred to a 96-well plate. For the positive control, 15 µL of Sdh positive control was taken into desired well(s) and the final volume was adjusted to 50 µL with Sdh assay buffer. Dichlorophenolindophenol (DCIP) standard 0, 4, 8, 12, 16, and 20 µL of 2 mM solution was added into a series of wells to generate 0, 8, 16, 24, 32, and 40 nmol/well of DCIP standard. The volume was adjusted to 100 µL per well with Sdh assay buffer. The reaction mixture of 50 µL was prepared to contain 46 µL

SDH assay buffer, 2 µL Sdh substrate mix, and 2 µL Sdh probe. The reaction mixture of 50 µL was added to each well containing the samples and positive control and mixed well. The absorbance was measured spectrophotometrically immediately at 599 nm in kinetic mode for 2 h at 25 ºC. Three replicates for each treatment were used and the experiment was conducted three times. The standard reading was subtracted from all the readings. The Sdh activity of the test sample was calculated as follows:

$$\Delta OD = A1 - A2$$

The ΔOD was applied to the DCIP standard curve to get "B" nmoles of DCIP reduced during the reaction time (ΔT = T2 – T1). The activity of mined compounds (AS) was measured as follows:

$$\mathrm{AS} = \frac{[B]\ x\ [\text{Dilution factor}]}{[(\Delta \mathrm{T}\ x\ V)]}$$

Where: B = Amount of reduced DCIP from standard curve (nmol), ΔT = Reaction time (min), V = Sample volume added into the reaction well (µL), D = Dilution factor. The activity was expressed as nanomoles of DCIP reduced in 1 min per mg protein.

2.3 *In vitro* conidial germination assay for mined compounds on FCO strains

The potential of the compounds to inhibit conidia germination was evaluated as previously described in Pasche et al. (2004), by comparing the conidial germination on water agar plates amended with or without the compounds. The spore suspension was prepared by flooding the plates with 5 mL water and the mycelial mat was gently rubbed to dislodge the conidia. The conidial suspension was then filtered through a nylon mesh (43 mm pore diameter) and adjusted to 1×10^5 conidia/mL using a hemocytometer. The compounds and pure technical grade penthiopyrad (positive control) were used to amend the agar plates at a concentration of 3 µg/mL. The control was amended with DMSO (1% v/v) with final concentration of 0.1 % (v/v). The aliquots (50 µL) of the conidial suspensions of the *F. oxysporum* (1×10^5 conidia/mL) were spread on fungicide-amended and fungicide-free Petri dishes (9 cm) with a glass rod.

The plates were incubated at 25 ± 1 ºC under continuous light for 4 h and 50 conidia/plate were examined for the development of germ tube. The conidium was considered germinated either when the germ tube was equal (or greater) in length as conidium diameter or if multiple germ tubes were emerging from one conidium. Three replicates were used for each treatment and the experiment was repeated three times. Inhibition percentage (PI) was calculated using the formula by Leroux and Gredet (Leroux and Gredet 1998), as follows:

$$PI = \frac{100(C - T)}{C}$$

Where C is the average conidia germinated in the control plate and T is the average conidia germinated in the treated plate.

2.4 *In vitro* mycelial growth assay against *F. oxysporum* f. sp. *capsici* strains

The food-poison technique was used (Pasche et al. 2004). Briefly, autoclaved PDA at 55 °C was amended with the compounds at 3 µg/mL and distributed in 9 cm diameter Petri dishes. The mycelial plugs (5 mm diameter) were cut from the margin of actively growing 5 days old culture on PDA and placed upside down in the center of fungicide-amended and non-amended PDA plates. The DMSO (0.1% v/v) amended plates served as negative control and the commercial fungicide penthiopyrad served as the positive control. The plates were incubated at 25 ± 1 ºC with 16 h of photoperiod for 7 days. Each treatment was triplicated, and the experiment was repeated three times. The diameter of each colony was measured by taking two perpendicular diameters from edge-to-edge of each colony after 7 days. Percentage inhibition (PI) of mycelial growth was computed as follows.

$$PI = \frac{100(C - T)}{C}$$

Where C is the mean diameter of the fungal colony (in cm) in the control plate and T is the mean diameter of the fungal colony (in cm) in the treated plate.

2.5 Statistical analysis

All data were pooled and subjected to One-Way or Two-Ways ANOVA analysis ($P < 0.05$) in R STUDIO v3.5.2. For correlation and principal component analysis, performanceanalytics, factoextra, and ggplot2 packages were integrated into the R studio and used for data visualization.

3. Results

3.1 Structural overview of the homology model

The developed pipeline (Fig. 1) successfully generated 25 potential cohort of ShdIs of which 12 is not yet found in the commercial domain but reported herein (Table 1). The homology model of Sdh for *F. oxysporum* (FCO) showed two hydrophilic proteins and two trans-membrane proteins. The two hydrophilic proteins included flavin adenine dinucleotide (FAD) binding protein (Fp of subunit A or FCO–SdhA) and iron-sulfur protein (FCO-SdhB). The two trans-membrane proteins included large cytochrome b (CybL or subunit C) and small cytochrome b (CybS or subunit D). The model contained a total of six

trans-membrane helices (Fig. 2). In FCO–Sdh model, the soluble catalytic heterodimer was composed of subunit A (FCO–SdhA) in which FAD cofactor was added by superimposition onto the template of Sdh crystal structure of *Sus_scrofa* (PDB ID: 1ZOY). The subunit B (FCO–SdhB) contained three iron-sulfur clusters: [2Fe-2S], [4Fe-4S], and [3Fe-4S]. The 3D molecular structure of FCO-Sdh also contained one heme molecule. The overall 3D structure was “q” letter shaped comprising of a hydrophilic head and a hydrophobic multi-pass trans-membrane-anchor tail. There was no direct interaction between FCO-SdhA and the trans-membrane hydrophobic anchors. The contact surfaces between the four subunits were dominated by the hydrophobic interactions.

3.2 Model evaluation and validation of discovered molecule docking sites

The generated model of FCO-Sdh presented the specific signature of Sdh and exhibited structural features comparable to the template (PDB code: 1ZOY). The superimposed view of the template and FCO-Sdh model are shown (Fig. 2). The comparison of FCO-Sdh and template (PDB code: 1ZOY) showed consistency in the built model and good overlap. The RMSD values between chain A, B, C, and D of FCO-Sdh model vis-à-vis the template (1ZOY) was 0.563 ångström (Å), 0.108 Å, 1.044 Å, and 1.119 Å, respectively.

The quality and stereo-chemical properties of the built FCO–Sdh model and the subunits were scrutinized by PROCHECK Ramachandran plot. Ramachandran plot analysis of subunit FCO-SdhA showed 89.7% of amino acid residues within the most favored region, whereas one residue was found in the disallowed region (Supplementary Fig. S3; Table S2). The PROCHECK results of subunit FCO-SDHB indicated that 86.9 % of the residues have phi- and psi- angles falling in the most favored regions (Supplementary Fig. S3; Table S2). For subunit FCO-SdhC, Ramachandran statistics showed that 92.6 % of the residues were in most favored region, while no residue was found in the disallowed region (Supplementary Fig. S3; Table S2). In the case of subunit FCO-SdhD, only one residue was in the disallowed region with 88.2 % residues in the most favored region.

Based on molecular docking performed in 1-Click Docking tool (Mcule 2014), and Autodock Vina Configuration (Trott and Olson 2010) the best-fit pose with the lowest binding energy from initial molecular docking, and the binding affinity for SdhI with UQ is shown (Fig. 2). The compound C1 forms H-bond with Phe83 of chain C at 3.13 Å and a binding energy of -10.75 kcal/mol. The binding energy for compound C2 was -11.02 kcal/mol and it formed H-bond with Phe83 of chain C with bond length 2.89 Å. Compound C10 had a binding energy of -10.86 kcal/mol and H-bonded with Trp82 at 3.07 Å. The interaction analysis revealed that Phe83 and Trp82 are critical amino acid residues for ligand binding, while Leu73.C, Trp205.B, Trp204.B, Pro201.B, Tyr76.C, Trp82.C, Ser84.C, Trp88.C, and Ile91.C provided hydrophobic interactions to the ligands (Fig. 2 A, B, C). Amino acid residues forming strong hydrogen bond networks were found in subunit C (Table 2).

3.3 Discovered SdhIs differentially inhibit *s*uccinate dehydrogenase enzyme

It was found that all the virulent strains of *F. oxysporum* f. sp. *capsici* produced succinate dehydrogenase with activity ranging from 3.0 – 3.3 U/mL in the presence of DMSO (Fig. 3). This signified that all the resistant virulent FCO strains used in this study constitutively expressed Sdh for metabolism. All the discovered compounds differentially decreased the activity of FCO Sdh (Fig. 3A). A significant decrease in Sdh activity was observed for the compound C1 (1.77 U/mL; F= 113.1, $P < 0.05$, P = 0.00), C2 (1.75 U/mL; F= 113.1, $P < 0.05$, P = 0.00), C6 (1.86 U/mL; F= 113.1, $P < 0.05$, P = 0.00) and C10 (1.83 U/mL; F= 113.1, $P < 0.05$, P = 0.00) and relative to penthiopyrad (2.57 U/mL; F= 113.1, $P < 0.05$). The commercial fungicide penthiopyrad showed Sdh activity ranging from 2.26–3.03 U/mL against all the FCO isolates. For the other tested compounds, Sdh activity varied from 1.3 to 2.96 U/mL for all the isolates. To confirm the uniqueness of the resistant and virulent FCO strains used in this study, principal component analysis (PCA) based on their Sdh expression pattern generated two groups (Fig. 3B). Group one was composed of FCO2, FCO5, FCO8, FCO10 strains, and the principal component was 7.79%. Also, group two was composed of FCO1, FCO3, FCO4, FCO6, and FCO7 strains and the principal component was 69.4%. The diverse nature of FCO strains enriched the usefulness of the discovered compounds to effectively manage resistant and virulent FCO strains and relatives. PCA analysis revealed that the discovered SdhIs differentially inhibited *s*uccinate dehydrogenase enzyme of FCO strains (Fig. 3C).

3.4 Discovered SdhIs effectively inhibits germ tube germination

The compounds were evaluated against the resistant and virulent FCO strains at the spore level by *in vitro* conidial germination assay. The antifungal activity of the twelve tested compounds and reference control penthiopyrad (PEN) showed divergent important antifungal potential. Using R package PerformanceAnalystics, a correlation analysis was performed to determine the global performance of all the tested compounds to the various FCO strains with different degree of sensitivity (Fig. 4). Compound C1, C2, C6, C9, and C10 exhibited mean significant germ tube inhibition against all the strains of FCO. The inhibitory pattern of compounds C1 vs C2, C9 vs C10, C10 vs C12, and C9 vs C12 on all the FCO strains indicated a significant positive correlation (*$r = 0.67, P < 0.05$), (*$r = 0.65, P < 0.05$), (**$r = 0.77, P < 0.05$), (*$r = 0.71, P < 0.05$), respectively. The significance of these findings is that the discovered compounds with positive correlation could be used for formulation to generate a stronger synergistic effect to target spore germination whereas significant negative correlation could generate antagonistic effects, thus, low antifungal potential. The inhibitory pattern of compound C2 vs C6 and C3 vs C6 on all the FCO strains indicated positive correlation ($r = 0.51, P < 0.05$) and ($r = 0.62, P < 0.05$), respectively.

3.5 Discovered SdhIs effectively inhibit FCO mycelial growth *in vitro*

To confirm whether the molecule's inhibitory pattern at the mycelial level was akin to that observed at the germ tubes, a PCA analysis was performed. Two strong principal components generated were 87.9% and 3.2% (Fig. 5A). The FCO strains clustered into two groups vis-à-vis the active compounds as observed with germ tube assay (Fig. 5A). Cluster I consisted of FCO4, FCO5, FCO6, FCO8, and FCO10, and cluster II consisted of FCO9 and FCO3, and a singleton FCO2 (Fig. 5A). This clustering pattern differed from those of germ tube assay signifying that the compounds affect the physiology of the fungi differently at unique

growth stages. Furthermore, it was observed from the PCA analysis that the most active compounds (C1, C2, and C10) formed cluster III and were active against all the FCO strains (Fig. 5A).

Mycelial growth inhibition of the twelve compounds was evaluated against the ten virulent *F. oxysporum* isolates on PDA medium. All the tested compounds effectively reduced the linear mycelial growth of all the isolates at 3 µg/mL relative to control (Supplementary Table S3). Differential level of mycelial growth inhibition was observed for the molecules relative to all the FCO strains. The compounds C6 and C10 were highly active against FCO mycelial growth hallmarked by 89.5% and 88.6% inhibition while compound C11 was least potent with 64.5% inhibition. The compound C1 was found the most effective exhibiting mycelial growth inhibition at 88.33% for FCO1, 87.33% for FCO2, 86.33% for FCO3, 87.33% for FCO6, 86.33% for FCO7, and 87.67% for FCO8. The compound C6 also showed strong mycelial inhibition of 89.50% for FCO4, 86.67% for FCO9, and 85.67% for FCO10 (Fig. 6). The rest of the compounds were relatively less effective in controlling all the resistant and virulent FCO strains (Supplementary Table S3).

4. Discussion

The *Fusarium* wilt of chili pepper caused by *Fusarium oxysporum* f. sp. *capsici* is a serious threat to chili farming and food safety. Based on a worldwide survey and the economic impact, *F. oxysporum* was voted by plant pathologist as the 5th most significant fungal pathogen (Dean et al. 2012). This has led to the deployment of transgenic resistant plants (Gaspar et al. 2014), the use of crop rotation, cultural techniques, biological control, and chemical control methods in many chili farming regions to manage *Fusarium* wilt. Because chemical control strategy provided both protective and curative solutions, most Pakistani farmers have opted for fungicides to enhance production and revenue, thus, the need to develop new fungicides.

In the present study, the application of integrated computational drug designing (Fig. 1) approach combined with structure-based virtual screening (SBVS), docking, and scoring was used to identify lead compounds with previously untested molecular scaffolds as succinate dehydrogenase inhibitors (SdhIs). The Sdh enzyme catalyzes the oxidation of succinate to fumarate and the reduction of ubiquinone (UQ) to ubiquinol (QH2). The competitive inhibition of Sdh by antifungal compounds prevent the reduction of UQ, interrupting the mitochondrial ETC, and shutting down the TCA cycle. Thus, this leads to a rapid decrease of cellular ATP levels (Matsson and Hederstedt 2001; Glättli et al. 2009). This mode of action enables the antifungal compounds to exert highly effective and selective control of fungal growth and development. In this study, the Sdh 3D homology model (Fig. 2) exhibited an analogous allocation of the main secondary structure and well superimposed but few loops and turns showed some structural deviations (Supplementary Fig. S3). This is not unforeseen, since the secondary structure is well conserved and has fewer amino acid insertions and deletions than the loop regions (Fig. 2). The SdhA and SdhB of FCO showed high sequence homologies with template subunit A (GenBank: EXL62804.1), B (GenBank: EXL48360.1), C (GenBank: SCO81136.1), and D (GenBank: EXL44012.1). These results are in line with Burger et al. (Burger et al. 1996), and Adams et al. (Adams et al. 2001), who reported that the amino acid sequences of Sdh1 and Sdh2 have 80% homology among eukaryotes at the binding site. In

FCO model of Sdh, the subunits SdhC and SdhD showed low sequence homology with that of *A. alternata* (Avenot et al. 2008).

Intriguingly, we found that the UQ binding site in FCO model of Sdh is a hydrophobic pocket that comprised of residues from SdhB, SdhC, and SdhD (Leu73.C, Trp205.B, Trp204.B, Pro201.B, Tyr76.C, Trp82.C, Ser84.C, Trp88.C, and Ile91) (Fig. 2) which corresponds to the findings in Horsefield et al (2006). Frequent mutations have been recognized in the Sdh at different positions in subunits B, C, and D notably in field isolates of *Alternaria* and *Botrytis* species (Avenot et al. 2008; Veloukas et al. 2011), thus, reducing the efficacy of SdhIs (Scalliet et al. 2012; Sierotzki et al. 2013; FRAC 2017). Resistance against SdhIs has become a common phenomenon in many plant fungal pathogens of chili pepper in Pakistan (Khan et al. 2017; Nawaz et al. 2018b; Khaleeque and Khan 1991, Siddiqui and Akhtar 2007). Based on *in silico* analysis, we found that the binding modes of the discovered SdhI compounds were through the formation of hydrogen bonds with either Phe83 and/or Trp82. This signified that the residues are vital in stabilizing the ligands in the UQ site of FCO of model Sdh (Fig. 2). These results agree with those of Shimizu et al. (Shimizu 2012), who reported that rhodoquinone (RQ) site is surrounded by conserved residues (C-Ser72, C-Arg76, D-Asp106, and D-Tyr107) and involved in H-bond networks with RQ. We found from docking that the 12 selected SdhIs compounds bound to Sdh protein and block the active site.

One modeling strategy to enhance disease control and limit the risk of resistance development is to integrate novel fungicides with structural diversity into a spray program (Staub 1991). Amongst various drug screening approaches, *in silico* virtual screening is the most practical tool to screen enormous chemical libraries owing to a relatively minimal effort, low cost and have the potential to discover innovative drug candidates (Schapira et al. 2000; Shoichet 2004). The activity of the discovered SdhIs on FCO was accessed *in vitro* by Sdh enzyme activity assay (Fig. 3), conidia germ tube inhibition (Fig. 4), and mycelial growth inhibition assays (Fig. 5). The enzymatic inhibition varied from (3.0 – 3.3 U/mL) among all the tested molecules (Fig. 3). This suggested that the molecules formed different numbers and intensity of H-bonds at the UQ binding pocket of FCO Sdh translated by the formation of two principal components (7.79% and 69.74%) in the clustering analysis (Fig. 3B). These results are similar to previous studies for the interaction of carboxin with Sdh in *Botrytis cinerea* (Fritz et al. 1993). The positive results prompted the evaluation of the efficacy of the compound to inhibit germ tube development *in vitro* (Fig. 4). Importantly, strong positive correlation between C1 vs C2 (*r* = 0.67*), C9 vs C10 (*r* = 0.65*), and C10 vs C12 (*r** = 0.77*) are promising indications of the synergistic effects should they be use in combination against diverse FCO strains in disease management.

Using a predefined discriminatory dose of penthiopyrad (3 µg/mL) for assessing the sensitivity of FCO strains, significant and varied mycelial growth inhibition was obtained (Fig. 5, 6). It is possible, that the significant differences in mycelial growth inhibition could be due to variations in the degree of hydrophobicity (or hydrophobicity), penetration strength over the cell wall and cell membrane, SdhIs solubility in the fungal cell protoplasm, and inherent differences in the respiratory system of each fungal strain. Variations in mycelial antifungal effects of fungicides in *Fusarium* species are a common phenomenon. For instance, Peters et al. (Peters et al. 2008), showed that reference strains of *Fusarium*

coeruleum and F. sambucinum were sensitive to fludioxonil, but all field test strains of *F.* coeruleum and F. sambucinum were resistant to fludioxonil hallmarked by no growth inhibition at 100 mg/L. All the tested compounds actively reduced mycelial growth of FCO at 3 µg/mL as compared to the negative control (Fig. 6). In this present study, C2 (at 3 µg/mL) was found to be the most effective compound against all the FCO strains. This finding is in harmony with the ability of compound C2 to form multiple hydrophobic interactions with Trp69, Trp82, Tyr76, and Trp205 at the active site of FCO Sdh enzyme than the other compounds (Supplementary Fig. S4). Also, the positive correlation of C1 vs C2 (*r* = 0.67*), C9 vs C10 (*r* = 0.65*), and C10 vs C12 (*r** = 0.77*) on germ tube germination inhibition provides wider possibilities for exploiting the synergistic potential of the discovered compounds. Thus, signifying that the discovering of all these SdhIs could be used for the effective control of a wide range of *Fusarium oxysporum* strains.

5. Conclusion

In this study, we have integrated computational drug designing (CADD) to accelerate the discovery of structurally diverse antifungal lead compounds that could mitigate the ongoing FCO resistance in Pakistan. The discovered compounds displayed better control of FCO by forming strong conformational binding and provide enhanced antifungal activity effect. Without diversity in fungicide products readily available to farmers in the future, the gains to continue in business and produce adequate food would be threatened. Importantly, compounds C1, C2, C6, and C10 showed high potential to control *Fusarium* wilt of chili. Furthermore, the compounds identified in the present research work can function as new promising SdhI inhibitors and can be used as a starting point for the fungicide formulation, greenhouse and field trials, and prospective integration into pesticide spray programs.

Declarations

Conflict of Interest Statement

The authors declare that the research was conducted in the absence of any commercial or financial relationships that could be construed as a potential conflict of interest.

Acknowledgments

We are deeply grateful to Higher Education Commission, Pakistan. The research was supported by the grant from the HEC Pakistan.

Funding

This work was financially supported by Higher Education Commission, Pakistan.

Data availability

The data that support the findings of this study are available from the corresponding author upon reasonable request.

Ethics approval This article does not contain any studies with human participants or animals performed by any of the authors.

References

Adams KL, Rosenblueth M, Qiu YL, Palmer JD (2001) Multiple losses and transfers to the nucleus of two mitochondrial succinate dehydrogenase genes during angiosperm evolution. Genetics 158:1289–1300. https://doi.org/10.1093/genetics/158.3.1289

Agrios GN (2005) Plant Pathology. 5 edition. Elsevier Academic Press. London.

Avenot HF, Sellam A, Karaoglanidis G, Michailides TJ (2008) Characterization of mutations in the iron-sulphur subunit of succinate dehydrogenase correlating with boscalid resistance in *Alternaria alternata* from California pistachio. Phytopathol 98:736–42. https://doi.org/10.1094/PHYTO-98-6-0736

Bashir MR, Atiq M, Sajid M, Mohsan M, Abbas W, Alam MW, Bashair M (2017) Antifungal exploitation of fungicides against *Fusarium oxysporum* f. sp. *capsici* causing *Fusarium* wilt of chilli pepper in Pakistan. Env Sci Pollution Res 25:6797–6801. https://doi.org/10.1007/s11356-017-1032-

Burger G, Lang BF, Reith M, Gray MW (1996) Genes encoding the same three subunits of respiratory complex II are present in the mitochondrial DNA of two phylogenetically distant eukaryotes. Proc Nat Aca Sci 93:2328–2332. https://doi.org/10.1073/pnas.93.6.2328

Camacho C, Coulouris G, Avagyan V, Ma N, Papadopoulo J, Bealer K, Madden TL (2009) BLAST+: architecture and applications. BMC Bioinformatics 10 p.421. https://doi.org/10.1186/1471-2105-10-421

Dean R, Van Kan JA, Pretorius ZA, Hammond-Kosack KE, Di Pietro A, Spanu PD, Rudd JJ, Dickman M, Kahmann R, Ellis J, Foster GD (2012) The top 10 fungal pathogens in molecular plant pathology. Mol Plant Path 13:414–430. https://doi.org/10.1111/j.1364-3703.2011.00783.x

FRAC Fungicide Resistance Action Committee (2017) FRAC Code List ©*2017: Fungicides sorted by mode of action (including FRAC Code numbering). Fungicide Resistance Action Committee. Available at: <http://www.frac.info/docs/default-source/publications/frac-code-list/frac-code-list-2017-final.pdf?sfvrsn=2>. [Accessed 10th January 2017].

Fritz R, Lanen C, Drouhot V (1993) Effects of various inhibitors including carboxin on *Botrytis cinerea* mitochondria isolated from mycelium. Agronomie 13:225–230.

Gaspar YM, McKenna JA, McGinness BS, Hinch J, Poon S, Connelly AA, Anderson MA, Health RL (2014) Field resistance to *Fusarium oxysporum* and *Verticillium dahliae* in transgenic cotton expressing the plant defensin NaD1. J Exp Botany 66:1541–1550. https://doi.org/10.1093/jxb/eru021

Glättli A, Stammler G, Schlehuber S (2009) Mutations in the target proteins of succinate-dehydrogenase inhibitors (SDHI) and 14α-demethylase inhibitors (DMI.) conferring changes in the sensitivity-structural

insights from molecular modelling. In: 9th International Conference on Plant Diseases. Tours, France, 8-9 December 2009. France: Association Française de Protection des Plantes (AFPP), p.670–681.

Guex N, Peitsch MC (1997) SWISS-MODEL and the SwissPdbViewer: an environment for comparative protein modeling. Electrophoresis 18:2714–2723. https://doi.org/10.1002/elps.1150181505

Horsefield R, Yankovskaya V, Sexton G, Whittingham W, Shiomi K, Omura S, Byrne B, Cecchini G, Iwata S (2006) Structural and computational analysis of the quinone-binding site of complex II (succinate-ubiquinone oxidoreductase) A mechanism of electron transfer and proton conduction during ubiquinone reduction. J Biol Chem 281:7309–16. https://doi.org/10.1074/jbc.M508173200

Huang LS, Sun G, Cobessi D, Wang AC, Shen JT, Tung EY, Anderson V E, Berry EA (2006) 3-Nitropropionic acid is a suicide inhibitor of mitochondrial respiration that, upon oxidation by complex II, forms a covalent adduct with a catalytic base arginine in the active site of the enzyme. J Biol Chem 281:5965–5972. https://doi.org/10.1074/jbc.M511270200

Iftikhar S, Shahid AA, Halim SA, Wolters PJ, Vleeshouwers VGAA, Khan A, Al-Harrasi A, Ahmad S (2017) Discovering novel *Alternaria solani* succinate dehydrogenase inhibitors by in silico modeling and virtual screening strategies to combat early blight. Front Chem 5:100. https://doi.org/10.3389/fchem.2017.00100

Irum M (2007) Comparison of phytochemical and chemical control of *Fusarium oxysporum* f. sp. *cicera*. Mycopathologia 5:107–110.

Irwin JJ, Sterling T, Mysinger MM, Bolstad WS, Coleman RG (2012) ZINC: A free tool to discover chemistry for biology. RGJ Chem Inf Model 52, p.1757. doi:10.1021/ci3001277

Khaleeque MI, Khan SM (1991) Fungi associated with fruit rot and die-back diseases of chillies in Faislabad. Pak J Phytopathol 3:50–52.

Khan MTI, Ali Q, Ashfaq M, Waseem M (2017) Economic analysis of open field chilli (*Capsicum annuum* L.) production in Punjab, Pakistan. J Exp Biol Agri Sci 5:120–125. doi: 10.18006/2017.5(1).120.125

Laskowski RA, MacArthur MW, Moss DS, Thornton JM (1993) PROCHECK: a program to check the stereochemical quality of protein structures. J Appl Crystallogr 26(2). https://doi.org/10.1107/S0021889892009944

Leroux P, Gredet A (1988) Etude de l'activité des fongicides. INRA de Versailles.

Li Z, Wan H, Shi Y, Ouyang P (2004) Personal experience with four kinds of chemical structure drawing software: Review on ChemDraw, ChemWindow, ISIS/Draw, and ChemSketch. J Chem Inf Comput Sci 44:1886–1890. https://doi.org/10.1021/ci049794h

Matsson M, Hederstedt L (2001) The carboxin-binding site on *Paracoccus denitrificans* succinate: quinone reductase identified by mutations. J Bioenergetics Biomembranes 33:99–105. https://doi.org/10.1023/A:1010744330092

Morris GM, Huey R, Lindstrom W, Sanner MF, Belew RK, Goodsell DS, Olson AJ (2010) AutoDock4 and AutoDockTools4: Automated Docking with Selective Receptor Flexibility. J Comput Chem 30:2785–2791. https://doi.org/10.1002/jcc.21256

Nawaz k, Shahid AA, Bengyella L, Subhani MN, Ali M, Anwar W, Iftikar S, Ali SW (2018a) Evidence of genetically diverse virulent mating types of *Phytophthora capsici* from *Capsicum annum* L. World J Microb Biotech 34:130. https://doi.org/10.1007/s11274-018-2511-y

Nawaz k, Shahid AA, Bengyella L, Subhani MN, Ali M, Anwar W, Iftikar S, Ali SW (2018b) Diversity of *Trichoderma* species in chili rhizosphere that promote vigor and antagonism against virulent *Phytophthora capsici*. Scientia Horticulturae 239:242–252. https://doi.org/10.1016/j.scienta.2018.05.048

Pasche J, Wharam C, Gudmestad N (2004) Shift in sensitivity of *Alternaria solani* in response to Qoi fungicides. Plant Dis 88:181–187. https://doi.org/10.1094/PDIS.2004.88.2.181

Patel VK (2014) An economic analysis of production and marketing of chili (*Capsicum annuum* L.) in Raigarh district of Chhattisgarh. M.Sc. thesis submitted to the Department of Agricultural Economics, College of Agriculture, Raipur, India.

Peters RD, Platt HW, Drake KA, Coffin RH, Moorehead S, Clark MM, Al-Mughrabi KI, Howard RJ (2008) First Report of fludioxonil-resistant isolates of *Fusarium* spp. causing potato seed-piece decay. Plant Dis 92:172. https://doi.org/10.1094/PDIS-92-1-0172A

Remmert M, Biegert A, Hauser A, Söding J (2011) HHblits: lightning-fast iterative protein sequence searching by HMM-HMM alignment. Nat Methods 9:173–178. https://doi.org/10.1038/nmeth.1818

Scalliet G, Bowler J, Luksch T, Kirchhofer-Allan L, Steinhauer D, Ward K, Niklaus M, Verras A, Csukai M, Daina A, Fonne-Pfister R (2012) Mutagenesis and functional studies with succinate dehydrogenase inhibitors in the wheat pathogen *Mycosphaerella graminicola*. PLos One 7:e35429. https://doi.org/10.1371/journal.pone.0035429

Schapira M, Raaka BM, Samuels HH, Abagyan R (2000) Rational discovery of novel nuclear hormone receptor antagonists. Proc Nat Aca Sci 97:1008–1013. https://doi.org/10.1073/pnas.97.3.1008

Shimizu H, Osanai A, Sakamoto K, Inaoka DK, Shiba T, Harada S, Kita K (2012) Crystal structure of mitochondrial quinol–fumarate reductase from the parasitic nematode *Ascaris suum*. J Biochem 151:589–592. https://doi.org/10.1093/jb/mvs051

Shoichet BK (2004) Virtual screening of chemical libraries. Nature 432:862–865. https://doi.org/10.1038/nature03197

Siddiqui ZA, Akhtar MS (2007) Biocontrol of a chickpea root-rot disease complex with phosphate-solubilizing microorganisms. J Plant Path 89:67–77. https://www.jstor.org/stable/41998358

Sierotzki H, Scalliet G (2013) A review of current knowledge of resistance aspects for the next-generation succinate dehydrogenase inhibitor fungicides. Phytopathol 103:880–887. https://doi.org/10.1094/PHYTO-01-13-0009-RVW

Skaggs R, Decker MF, VanLeeuwen D (2000) A Survey of Southern New Mexico Chile Producers: Production, Practices and Problems. Las Cruces, NM: New Mexico State University, Agricultural Experiment Station. 782, p. 68.

Staub T (1991) Fungicide resistance: practical experience with antiresistance strategies and the role of integrated use. Ann Rev Phytopathol 29:421–442. https://doi.org/10.1146/annurev.py.29.090191.002225

Sun F, Huo X, Zhai Y, Wang A, Xu J, Su D, Bartlam M, Rao Z (2005) Crystal structure of mitochondrial respiratory membrane protein complex II. Cell 121:1043–1057. https://doi.org/10.1016/j.cell.2005.05.025

Thomas VC, Sadykov MR, Chaudhari SS, Jones J, Endres JL, Widhelm TJ, Ahn JS, Jawa RS, Zimmerman MC, Bayles KW (2014) A central role for carbon-overflow pathways in the modulation of bacterial cell death. PLoS Pathogens 10:e1004205. https://doi.org/10.1371/journal.ppat.1004205

Trott O, Olson AJ (2010) AutoDock Vina: improving the speed and accuracy of docking with a new scoring function, efficient optimization and multithreading. J Comput Chem 31:455–61. https://doi.org/10.1002/jcc.21334

Veloukas T, Leroch M, Hahn M, Karaoglanidis GS (2011) Detection and molecular characterization of boscalid-resistant *Botrytis cinerea* isolates from strawberry. Plant Dis 95:1302–1307. https://doi.org/10.1094/PDIS-04-11-0317

Tables

Table 1 Twelve compounds selected as novel SdhIs with their ZINC ID, common names, molecular weight, and codes.

No.	ZINC ID	Common names	Molecular Weight (g mol^{-1})	Unique Code name
1	ZINC00781454	(Z)-2-cyano-3-(4-isoindolin-2-ylphenyl)-N-(2-thenyl)acrylamide	385.492	C1
2	ZINC04498541	N-benzyl-2-cyano-3-(4-pyrrolidin-1-ylphenyl)-prop-2-enamide	331.419	C2
3	ZINC27260697	3-[(2-chlorobenzoyl)amino]-N-(3-cyano-4,5-dimethyl-2-thienyl)benzamide	409.898	C3
4	ZINC02409017	4-cyano-5-[[3-(2-ketochromen-3-yl)benzoyl]amino]-3-methyl-thiophene-2-carboxylic-acid-ethyl-ester	458.495	C4
5	ZINC00689200	2-amino-4-(3-bromophenyl)-1-(2-cyanophenyl)-5-oxo-1,4,5,6,7,8-hexahydro-3-quinolinecarbonitrile	446.328	C5
6	ZINC03102709	[4-bromo-2-[(2-hydroxy-2-phenyl-acetyl)aminoiminomethyl]phenyl]	453.292	C6
7	ZINC05176439	N-[3-[(2-hydroxy-3-methoxy-phenyl)methyleneaminocarbamoyl]phenyl]-2-methyl-benzamide	403.438	C7
8	ZINC06183077	(2Z)-3-(5-chlorothiophen-2-yl)-2-cyano-N-(1-phenylethyl)prop-2-enamide	316.813	C8
9	ZINC06512448	(2Z)-3-(4-tert-butylphenyl)-2-cyano-N-(pyridin-2-ylmethyl)prop-2-enamide	319.408	C9
10	ZINC17007371	N-(2-chloro-3-methylphenyl)-2-cyano-2-cyclopentylideneacetamide	274.751	C10
11	ZINC32180696	(Z)-N-benzyl-2-cyano-3-[4-[(2-fluorophenyl)methoxy]phenyl]prop-2-enamide	386.426	C11
12	ZINC34378628	(2Z,4E)-2-cyano-5-phenyl-N-[(1S)-1-phenylethyl]penta-2,4-dienamide	302.377	C12

Table 2 Interaction details of the most active compounds and residues that initiated strong hydrogen bonding network.

Sdhi	Sdh subunits	Interacting amino acids	Residues forming strong hydrogen bond network
C1	C	Phe83	Phe83
	C	Ile91	
	C	Leu73	
	C	Trp82	
	C	Trp88	
	C	Ala87	
	D	Try134	
C2	C	Phe83	Phe83
	C	Trp69	
	C	Trp82	
	C	Tyr76	
	B	Trp205	
	C	Trp82	Trp82
C10	C	Phe83	
	C	Ser84	
	B	Pro201	
	C	Leu73	
	C	Trp82	
	C	Ile91	

Figures

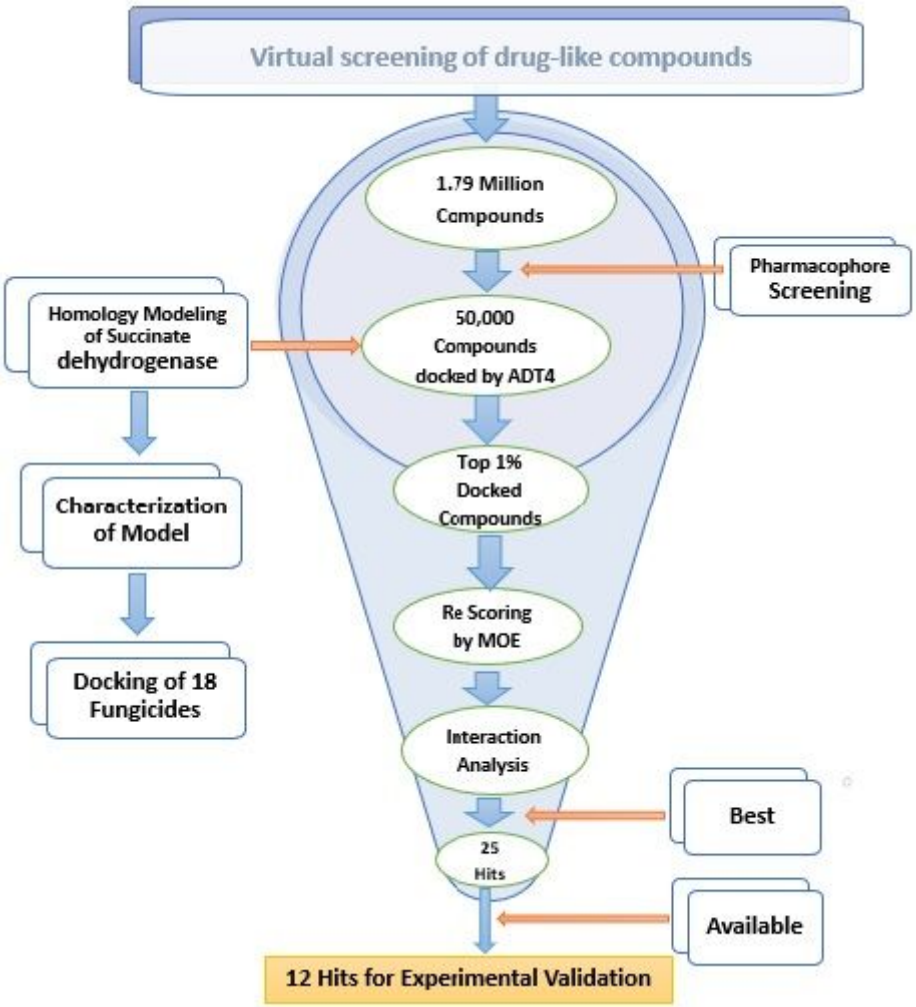

Figure 1

A pipeline for in silico discovery of SdhIs targeting UQ site for the management of Fusarium wilt of chili pepper.

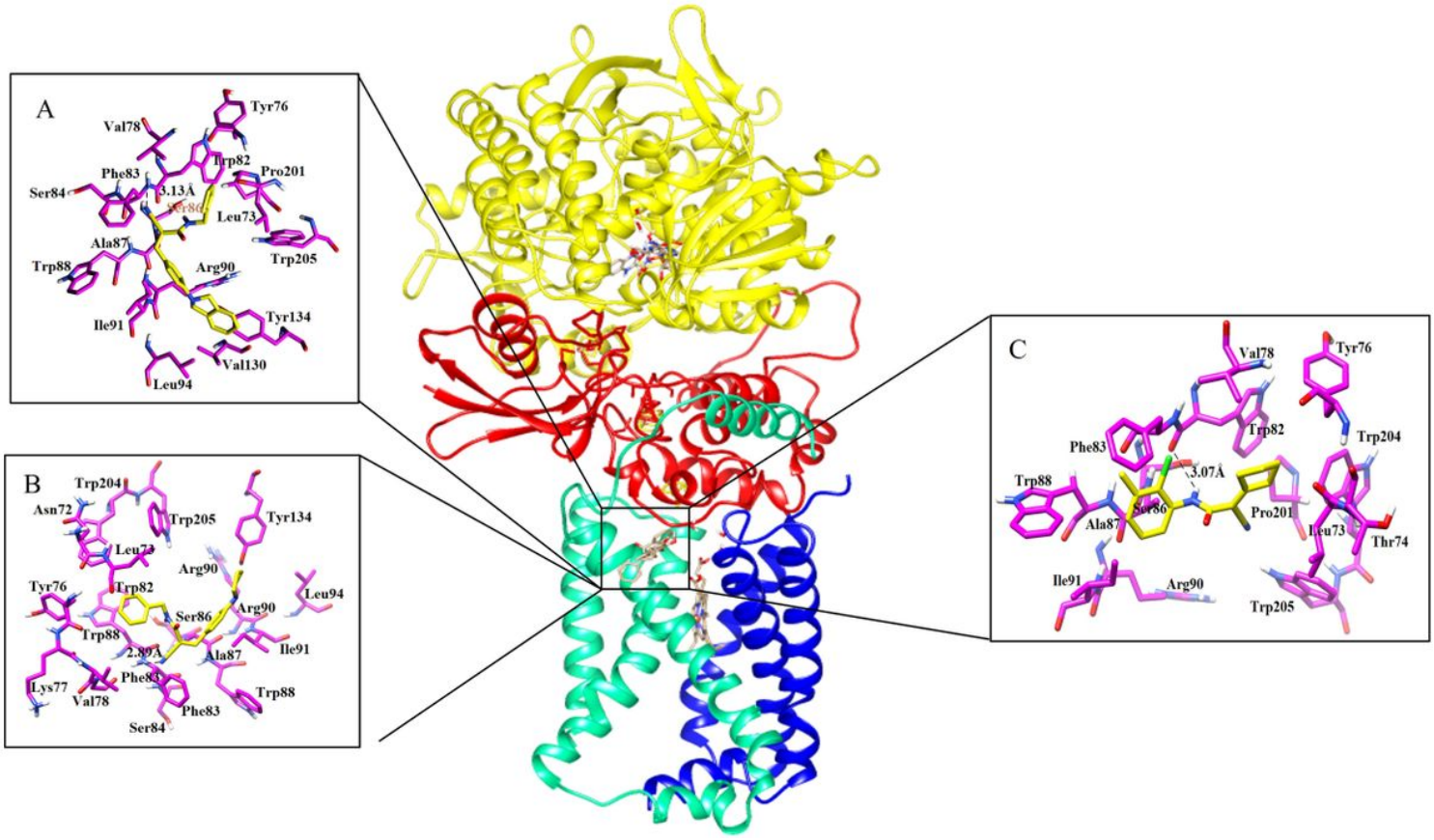

Figure 2

The docked orientation of C1, C2, and C10 SdhIs. The interacting residues and the compounds are presented in magenta and yellow stick colours, respectively. H-bonds are displayed in black dotted lines. (A) C1 (ZINC00781454), (B) C2 (ZINC04498541), (C) C10 (ZINC17007371).

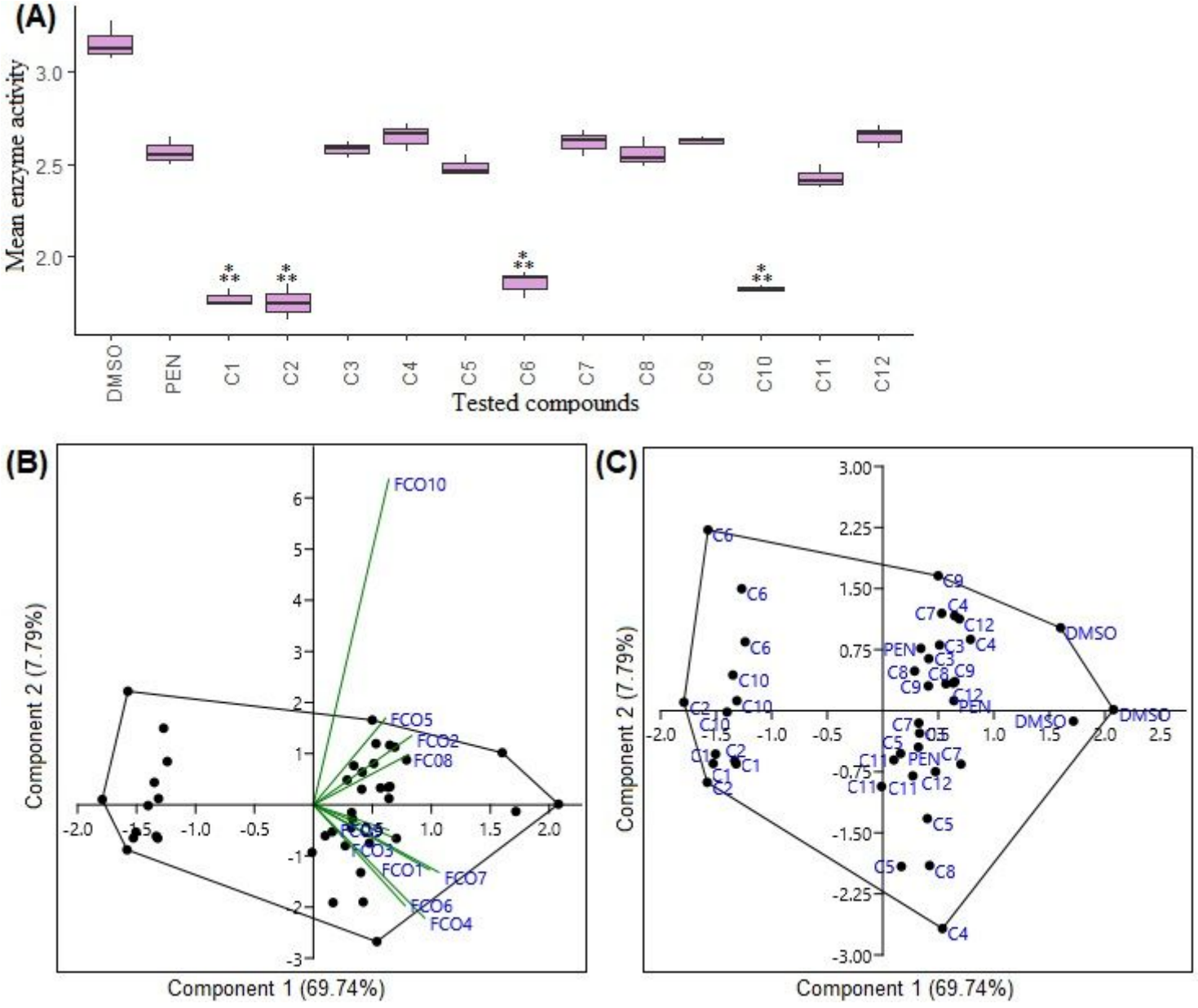

Figure 3

Specific inhibitory activity of tested compounds on FCO Sdh expression. (A) Mean decrease in Sdh activity (U/mL), and asterisks indicate levels of significant differences (*P < 0.05; **P < 0.001, ***P < 0.000). (B) Principal component analysis (PCA) biplot for the comparative distribution of studied F. oxysporum f. sp. capsici strains in function of their Sdh sensitivity to the tested compounds. (C) A PCA spanning–tree showing the activity map of the tested compounds relative to each FCO strains revealed the compounds have different bioefficacy. The analysis revealed that each compound has varied effect on different strains of F. oxysporum f. sp. capsici.

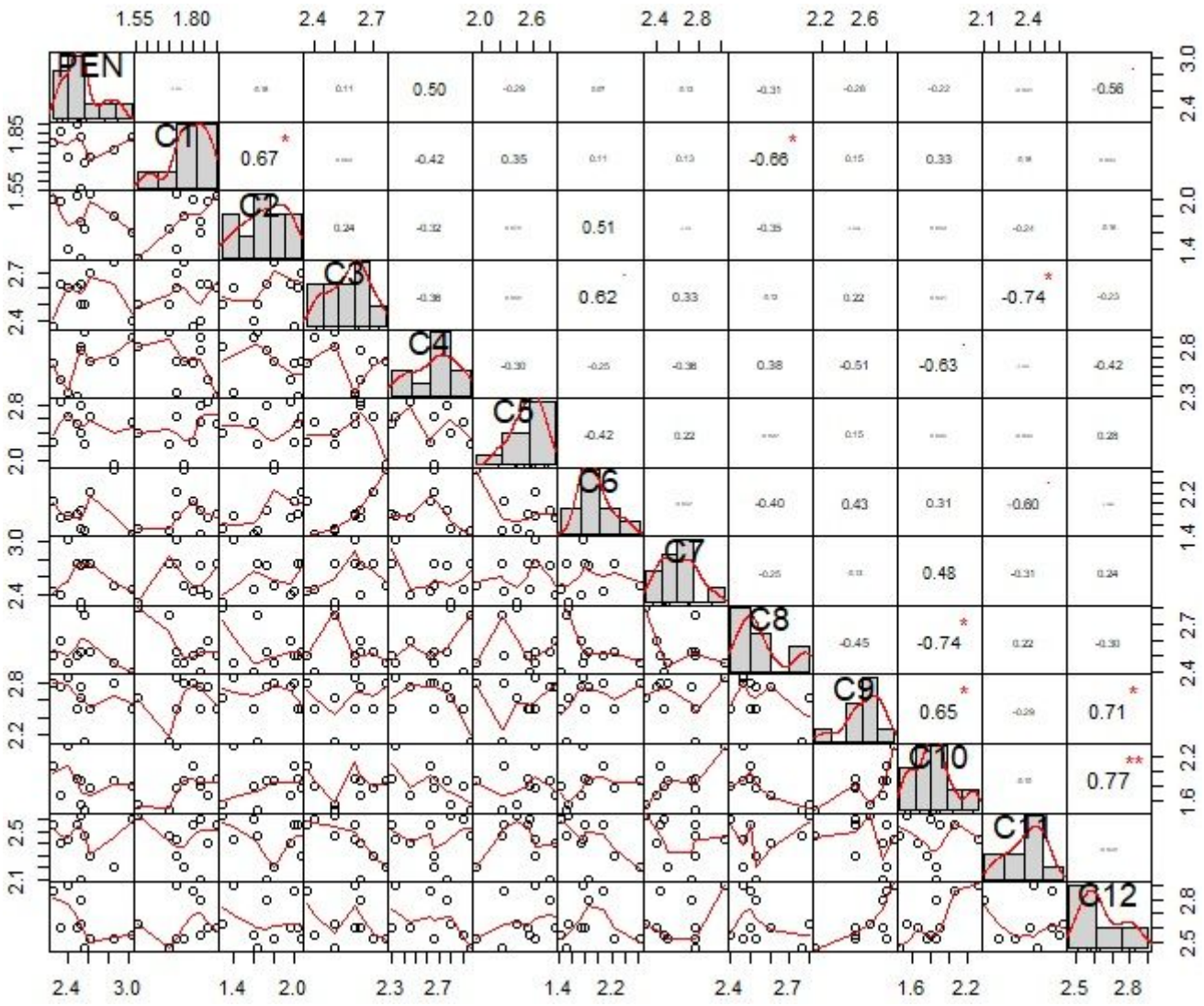

Figure 4

Pearson correlation coefficient (r) for germ tube inhibition by discovered compounds relative to commercial fungicide penthiopyrad on FCO strains. The asterisks indicate levels of significant differences (*r < 0.05; **r < 0.001, ***r < 0.000).

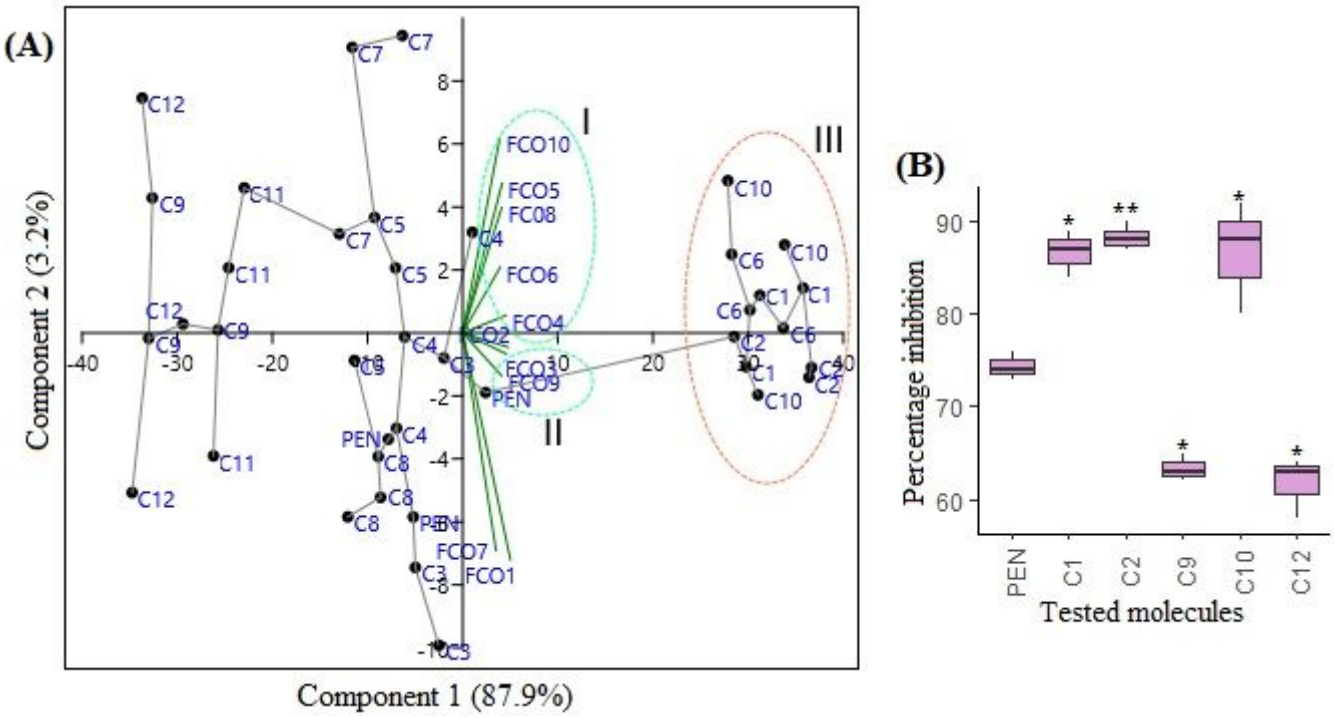

Figure 5

Compounds and mycelial growth inhibition. (A) Distribution of studied F. oxysporum f. sp. capsici strains in function of mycelial sensitivity to tested compounds. (B) Mycelial growth inhibition of the most active compounds on virulent FCO1 strain and the asterisks indicate levels of significant differences (*P < 0.05; **P < 0.001, ***P < 0.000).

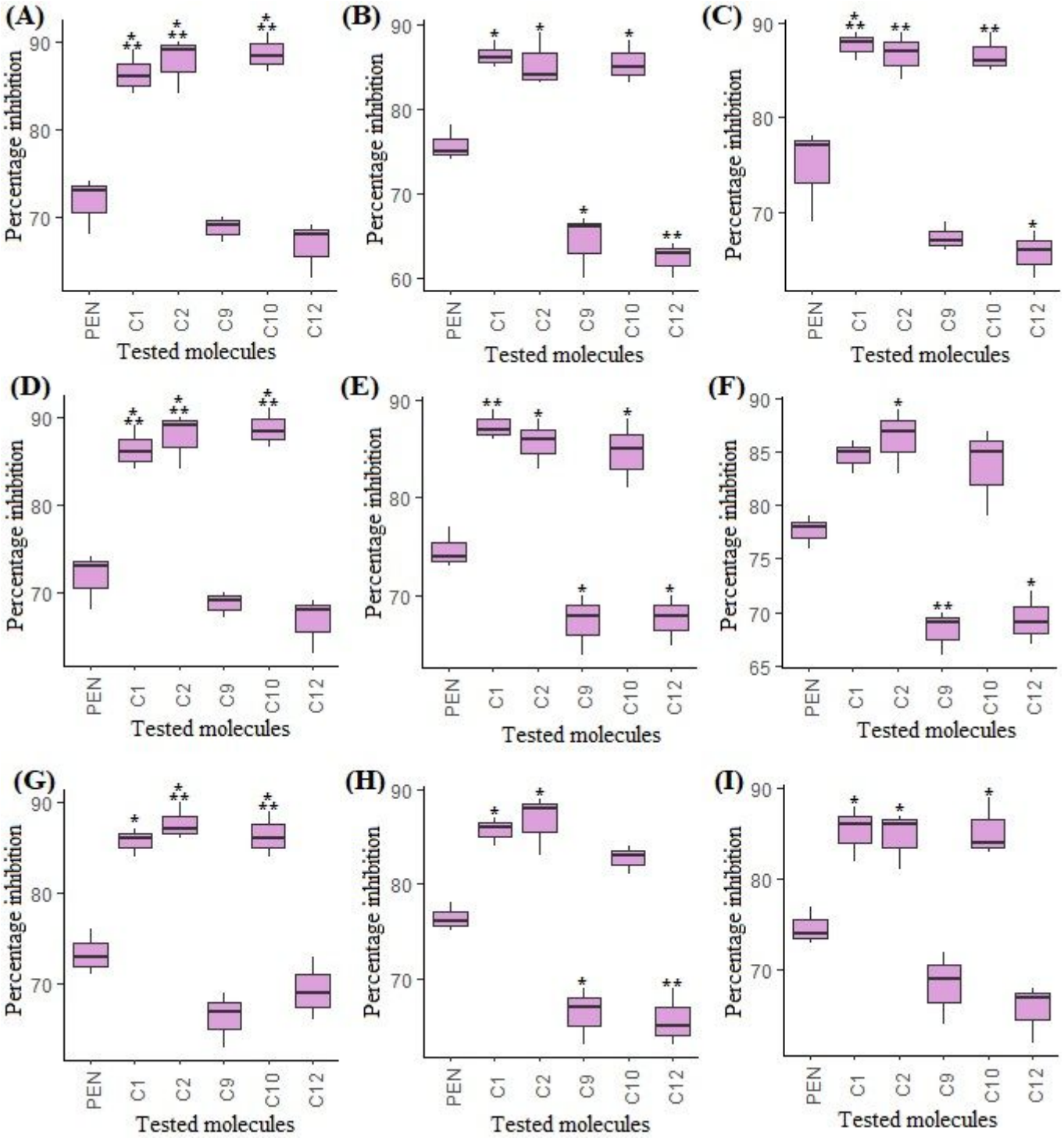

Figure 6

Mycelial growth inhibition of the most active compounds on virulent F. oxysporum f. sp. capsici strains. (A) FCO2, (B) FCO3, (C) FCO4, (D) FCO5, (E) FCO6, (F) FCO7, (G) FCO8, (H) FCO9, (I) FCO10 and the asterisks indicate levels of significant differences (*P < 0.05; **P < 0.001, ***P < 0.000).

Supplementary Files

This is a list of supplementary files associated with this preprint. Click to download.

- Supplementarymaterials.V2.pdf